

# Big but Imperceptible Adversarial Perturbations via Semantic Manipulation

Anand Bhattad\* Min Jin Chong\* Kaizhao Liang Bo Li David A. Forsyth  
University of Illinois at Urbana-Champaign

{bhattad2, mchong6, k12, lbo, daf}@illinois.edu

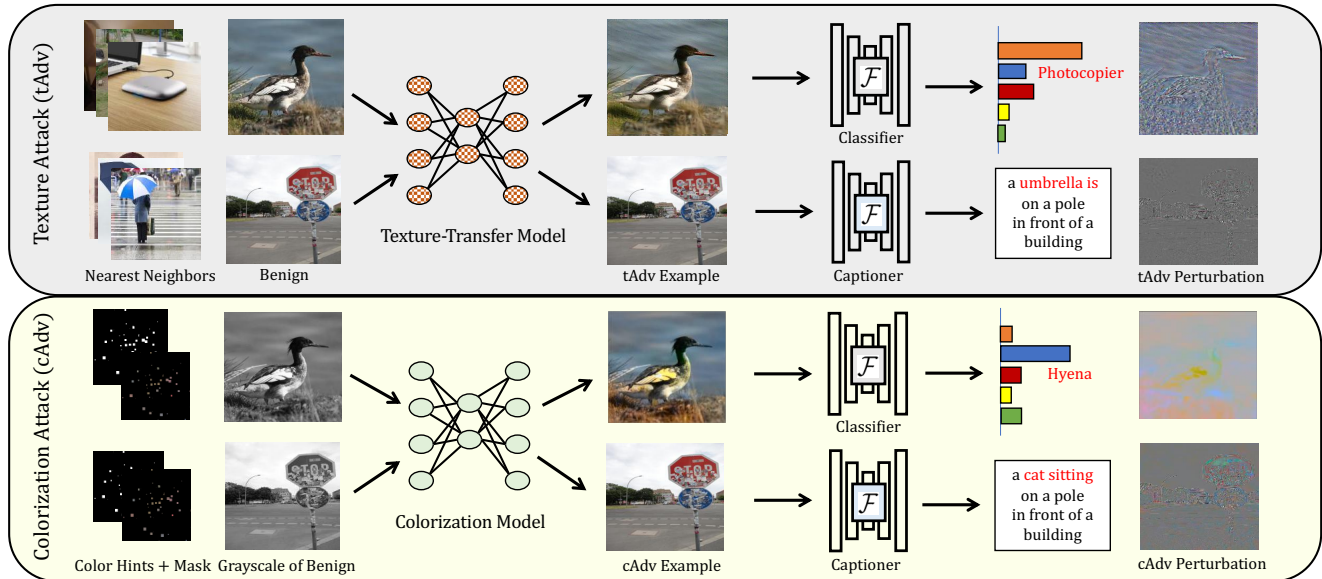


Figure 1: **Pipeline of proposed attacks.** **Top:** Texture transfer attack (tAdv); **Bottom:** Colorization attack (cAdv). Our attacks achieve high attack success rate via semantic manipulation of victim images without any constraints on  $\mathcal{L}_p$  norm.

## Abstract

Machine learning, especially deep learning, is widely applied to a range of applications including computer vision, robotics and natural language processing. However, it has been shown that machine learning models are vulnerable to adversarial examples, carefully crafted samples that deceive learning models. In-depth studies on adversarial examples can help better understand potential vulnerabilities and therefore improve model robustness. Recent works have introduced various methods which generate adversarial examples. However, all require the perturbation to be of small magnitude ( $\mathcal{L}_p$  norm) for them to be imperceptible to humans, which is hard to deploy in practice. In this paper we propose two novel methods, tAdv and cAdv, which leverage texture transfer and colorization to generate natural perturbation with a large  $\mathcal{L}_p$  norm. We conduct extensive experiments to show that the proposed methods are general enough to

attack both image classification and image captioning tasks on ImageNet and MSCOCO dataset. In addition, we conduct comprehensive user studies under various conditions to show that our generated adversarial examples are imperceptible to humans even when the perturbations are large. We also evaluate the transferability and robustness of the proposed attacks against several state-of-the-art defenses.

## 1. Introduction

Machine learning (ML), especially deep learning, has achieved great successes in various tasks, including modeling, predicting and classifying large datasets. Recent literature have shown that these widely deployed ML models are vulnerable to adversarial examples – carefully crafted small perturbation aimed to mislead learning models [4, 22, 30]. Adversarial examples have caused many concerns mainly for security critical domains [3, 10]. Studying them is one important way to better understand such vulnerabilities and therefore develop robust ML models.

\* indicates equal contributions.

To date, many methods have been proposed to generate adversarial examples [14, 4, 22, 29, 30]. However, all these attack methods search for adversarial perturbation with small  $\mathcal{L}_p$  norm to appear invisible to humans, which is hard to deploy in practice. For instance, small  $\mathcal{L}_p$  norm perturbations will be difficult to be captured by cameras in the physical world and thus fail to be effective in real scenarios. In addition, such small perturbations can be fragile and simple operations such as JPEG or pixel quantization will be able to reduce its effectiveness. Furthermore, under certain scenarios (e.g. more complicated models), small perturbations are insufficient in achieving a high attack success rate. These weaknesses of existing adversarial perturbation motivate researchers to seek for solutions in generating perturbation with large  $\mathcal{L}_p$  norm which not only misleads learning models but also goes unnoticed by humans. In particular, Google has hosted a competition for generating “unrestricted adversarial examples” [1].

To achieve the goal of unrestricted adversarial examples, we propose two novel methods, tAdv and cAdv to construct adversarial examples that are “far” from the original image in  $\mathcal{L}_p$  norm, but look natural to humans. This is done through the manipulation of explicit semantic visual representations (e.g. texture; color). tAdv utilizes the texture from nearest neighbor instances and adjusts the instance’s texture field using style transfer as adversarial perturbation, while cAdv adaptively chooses locations in an image to change their colors, producing adversarial perturbation that is usually fairly substantial. Such semantic transformation-based adversarial perturbation sheds light upon the understanding of what information is important for neural networks to make predictions. For instance, in one of our case studies, we found that when the road is recolored from gray to blue, the image gets misclassified to tench (a fish) although a car remains evidently visible (Fig. 4b). This indicates that deep learning models can easily be fooled by certain local patterns. In addition to image classifiers, the proposed attack methods can be generalized to different machine learning tasks such as image captioning [2]. Our attacks can either change the entire caption to the target or take on more challenging tasks like changing one or two specific target words from the caption to a target. For example, in Fig. 1, “stop sign” of the original image caption was changed to “umbrella is” and “cat sitting” for tAdv and cAdv respectively.

To guarantee that our large adversarial perturbations are imperceptible to humans, we conducted extensive user studies under various conditions. We compare our generated adversarial examples with the ones based on the state of the art methods (e.g. Basic iterative method (BIM) [22] and optimization based attack [4]) and show that when the  $\mathcal{L}_p$  norm of the perturbation is small, all methods appear natural to humans. However, when we relaxed the bound on perturbation, as  $\mathcal{L}_\infty$  increases from 0.20 to 0.49, the pro-

posed methods stay imperceptible (user study score changes from 48% to 43%). In comparison, performances drop drastically for other attack methods (from 49% to 33%) as  $\mathcal{L}_\infty$  increases from 0.05 to 0.34.

We tested our proposed attacks on several state of the art defenses. Rather than just showing the attacks break these defenses (better defenses will come up), we aim to show that tAdv and cAdv are able to produce new types of adversarial examples which are more robust towards considered defenses than other attacks. Our proposed attacks are also more transferable given their large perturbation [26]. These new features of the proposed adversarial examples provide further insights into the vulnerabilities of learning models and therefore encourage new solutions to improve their robustness.

**Contributions:** 1) We describe two novel methods based on semantic transformation to generate adversarial examples; 2) Our attacks are unrestricted with no constraints on  $\mathcal{L}_p$  norm; 3) We conduct extensive experiments to attack both image classification and image captioning models on large scale ImageNet [7] and MSCOCO [24] dataset; 4) We perform comprehensive user studies under different scenarios to show that when compared to other attacks, our generated adversarial examples appear more natural to humans at large perturbation  $\mathcal{L}_p$  norm; 5) We test different adversarial examples against several state of the art defense methods and show that the proposed attacks are not only more robust but also contain unique properties.

## 2. Related Work

In this section, we will briefly summarize current approaches generating adversarial examples, and discuss several standard semantic image transformation approaches. **Adversarial examples** have attracted a lot of attention recently due to its interesting properties such as being “indistinguishable from benign images” to human perception. Currently, most adversarial perturbations are measured by  $\mathcal{L}_p$  norm distance. For instance, fast gradient sign method (FGSM) is proposed to add perturbation  $\epsilon$  with small norm distance to benign instance  $x$  (i.e. adversarial example  $x_{adv} = x + \epsilon$ ) with respect to the direction of gradient of target learning model  $f$  [14]. Optimization based attack optimizes  $\epsilon$  so that  $x_{adv}$  is misclassified to the adversarial target and the magnitude of  $\|\epsilon\|_p$  is minimized [4, 22]. Though the norm distance is not a perfect metric to measure similarity for images, current adversarial examples mostly rely on bounding the norm based distance to guarantee  $x_{adv}$  to be close to the benign instance and therefore appear “natural” to humans. Later, Xiao *et al.* proposed to change pixel positions instead of pixel values to generate adversarial examples. While this attack leads to “natural” looking adversarial examples with large  $\mathcal{L}_p$  norm, it does not take image semantic information into account [30]. Unlike previous

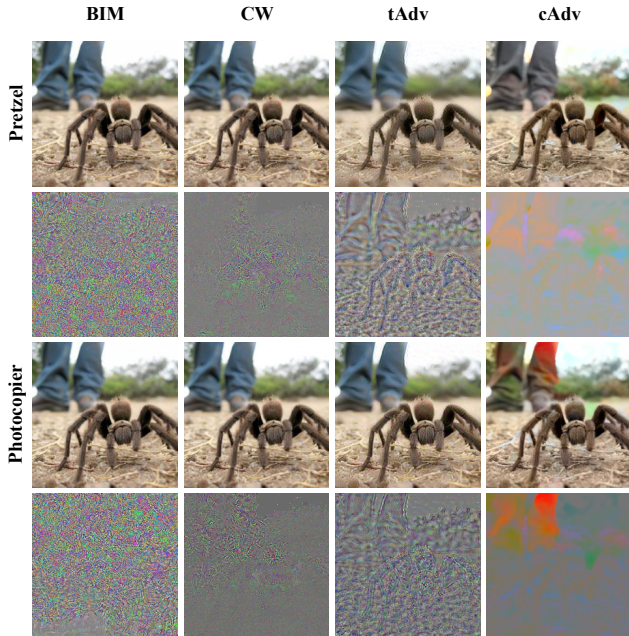


Figure 2: **Perturbation comparisons.** Images are attacked from tarantula to pretzel in the first row and photocopier in the third row. Our perturbations are large, structured and have spatial patterns when compared with other attacks. Perturbations from cAdv are low-frequency and locally smooth while perturbations from tAdv are primarily high-frequency and structured. Note gray color denotes zero perturbations.

attack methods, our attacks are unbounded while remaining realistic. They are also effective in attacking different machine learning models.

**Texture transfer** extracts texture from one image and adds it to another. Texture is one of the most crucial descriptors that aids image recognition [5]. Transferring texture from one source image to another target image has been widely studied in computer vision [9, 11]. The Convolutional Neural Network (CNN) based texture transfer from Gatys et al. [11] led to a series of new ideas in the domain of artistic style transfer [12, 18, 23, 32]. It was identified that within-layer feature statistics or gram matrices of a pretrained deep neural net extract strong texture cues from the image. Recently, Yeh et al. [32] demonstrated cross layer gram matrices are more effective in extracting texture than within-layer [12]

**Image Colorization** is the task of giving natural colorization to a grayscale image. This is an ill-posed problem as there are multiple viable natural colorizations given a single grayscale image. Deshpande et al. [8] showed that diverse image colorization can be achieved by using an architecture that combines VAE [21] and Mixture Density Network; while Zhang et al. [34] demonstrated an improved and diverse image colorization by using input hints from users guided colorization process.

### 3. Texture Attack (tAdv)

Our goal is to generate adversarial examples by infusing texture from another image without explicit constraints on  $\mathcal{L}_p$  norm of the perturbation. For generating our tAdv examples, we used a pretrained VGG19 network [27] to extract textural features [12]. We directly optimize our victim image ( $I_v$ ) by adding texture from a target image ( $I_t$ ). A natural strategy to transfer texture is by minimizing within-layer feature correlation statistics (gram matrices) between two images [11, 12]. Based on Yeh et al. [32], we found optimizing cross-layer gram matrices instead of within-layer gram matrices helps produce more natural looking adversarial examples. The difference between the within-layer and the cross-layer gram matrices is that for a within-layer, the features statistics are computed between the same layer. For a cross-layer, statistics are between two adjacent layers.

**tAdv Objectives.** tAdv directly attacks the image to create adversarial examples. Moreover, there is no additional content loss that is used in style transfer methods [12, 32]. Our overall objective function for the texture attack contains a texture transfer loss ( $L_t^A$ ) and an adversarial loss ( $J_{adv}$ ).

$$L_{tAdv}^A = \alpha L_t^A(I_v, I_t) + \beta J_{adv}(\mathcal{F}(I_v), t) \quad (1)$$

Unlike style transfer methods, we do not want the adversarial examples to be artistically pleasing. Our goal is to infuse a reasonable texture from a target class image to the victim image to fool a classifier or captioning network. To ensure a reasonable texture is added without perturbing the victim image too much, we introduce an additional constraint on the variation in the gram matrices of the victim image. This constraint helps us to control the image transformation procedure and prevents it from producing artistic images. Let  $m$  and  $n$  denote two layers of a pretrained VGG-19 with a decreasing spatial resolution and  $C$  for number of filter maps in layer  $n$ , our texture transfer loss is then given by

$$L_t^A(I_v, I_t) = \sum_{(m,n) \in \mathcal{L}} \frac{1}{C^2} \sum_{ij} \frac{\|G_{ij}^{m,n}(I_v) - G_{ij}^{m,n}(I_t)\|^2}{std(G_{ij}^{m,n}(I_v))} \quad (2)$$

Let  $f$  be feature maps,  $\mathcal{U}f^n$  be an upsampled  $f^n$  that matches the spatial resolution of layer  $m$ . The cross layer gram matrices  $G$  from [32] between the victim image ( $I_v$ ) and a target image ( $I_t$ ) is given as

$$G_{ij}^{m,n}(I) = \sum_p [f_{i,p}^m(I)] [\mathcal{U}f_{j,p}^n(I)]^T \quad (3)$$

**Texture Transfer.** To create tAdv adversarial examples, we need to find images to extract the texture from, which we call “texture source” ( $T_s$ ). A naive strategy is to randomly select an image from the data bank as  $T_s$ . Though this strategy is successful, their perturbations are clearly perceptible. Alternatively, we can randomly select  $T_s$  from the adversarial target class. This strategy produces less perceptible



Figure 3: **tAdv strategies.** Texture transferred from random “texture source” ( $T_s$ ) in row 1, random target class  $T_s$  (row 2) and from the nearest target class  $T_s$  (row 3). All examples are misclassified from *Beacon* to *Nautilus*. Images in the last row look photo realistic, while those in the first two rows contain more artifacts as the texture weight  $\alpha$  increases.

perturbations compared to the random  $T_s$  method as we are extracting a texture from the known target class. A better strategy to select  $T_s$  is to find a target class image that lies closest to the victim image in the feature space using nearest neighbors. This strategy is sensible as we assure our victim image has similar feature statistics as our target image. Consequently, minimizing gram matrices is easier and our attack generates more natural looking images (see Fig. 3).

**Control over Texture.** The extent of texture that gets added to our victim image is controlled by the texture weight coefficient ( $\alpha$ ). Increasing texture weights improves attack success rate at the cost of noticeable perturbation. When compared to within-layer statistics, the cross-layer statistics that we use are not only better at extracting texture, it is also easier to control the texture weight.

**Structured tAdv Perturbations.** Our tAdv perturbations are big when compared with existing attack methods in  $\mathcal{L}_p$  norm. They are of high-frequency and yet imperceptible (see Fig. 1 and Fig. 2). Since we are extracting features across different layers of VGG, the perturbations that we observe from tAdv examples follow a textural pattern. They are more structured and organized when compared to others.

## 4. Colorization Attack (cAdv)

In this section, our goal is to adversarially color an image by leveraging a pretrained colorization model. We hypothesize that it is possible to find a natural colorization that is adversarial for a target model (e.g., classifier or captioner) by searching in the color space. Since a colorization network learns to color natural colors that conform to boundaries and respect short-range color consistency, we can use it to introduce long-scale adversarial noise with a large magnitude that looks natural to humans. This differs from common



Figure 4: **Class color affinity.** cAdv on network weights with no provided hints. Groundtruth class for (a) is *pretzel*. The new colors are commonly found in images from target class. This gives us insights into the importance of colors as a factor in how classifiers make decisions.

adversarial attacks which tend to introduce short-scale high-frequency artifacts that are minimized to be invisible for human observers.

We leveraged Zhang *et al.*’s [33] colorization model for our attack. In their work, they produce natural colorization on the ImageNet dataset using input hints from the user. The inputs to their network consist of the L channel of the image in CIELAB color space  $X_L \in \mathbb{R}^{H \times W \times 1}$ , the sparse colored input hints  $X_{ab} \in \mathbb{R}^{H \times W \times 2}$ , and the binary mask  $M \in \mathbb{B}^{H \times W \times 1}$ , indicating the location of the hints.

**cAdv Objectives.** There are a few ways to leverage the colorization model to achieve adversarial objectives. We experimented with two main methods and achieved varied results.

**Network weights.** The straightforward method of producing adversarial colors is to change Zhang *et al.*’s colorization network  $\mathcal{F}$  directly. To do so, we simply update  $\mathcal{F}$  by minimizing  $J_{adv} \cdot t$  represents target class.

$$\theta^* = \arg \min_{\theta} J_{adv}(\mathcal{F}(X_L, X_{ab}, M; \theta), t) \quad (4)$$

**Hints and mask.** We can also vary input hints  $X_{ab}$  and mask  $M$ . Hints provides the network with ground truth color patches that guides the colorization while the mask provides its spatial location. By jointly varying both hints and mask, we are able to manipulate the output colorization. We can update our hints and mask as follows.

$$M^*, X_{ab}^* = \arg \min_{M, X_{ab}} J_{adv}(\mathcal{F}(X_L, X_{ab}, M; \theta), t) \quad (5)$$

**Attack Methods.** Attacking network weights allows the network to search the color space with no constraints for adversarial colors. This attack is the easiest to optimize, but the output colors are not realistic as shown in Fig. 4. Our various strategies outlined are ineffective as the model learns to ignore them and instead, directly generate the adversarial colors. However, the colorization it produces correlate with colors often observed in the target class. This suggests that classifiers associate certain colors with certain classes which we will discuss more in our case study.

Attacking input hints and mask instead gives us natural results as the pretrained network will not be affected by our optimization. Attacking hints and mask separately works,

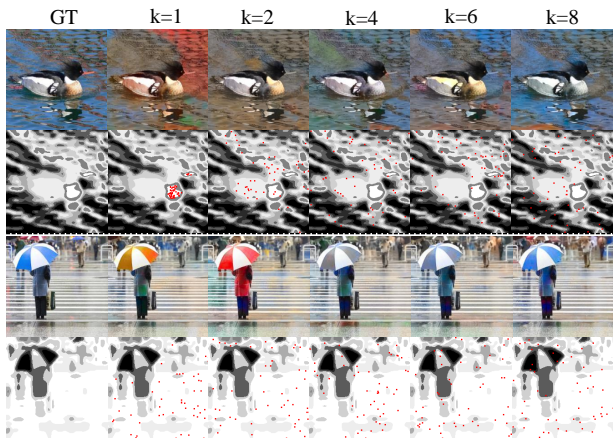


Figure 5: **Controlling cAdv.** We show a comparison of sampling 50 color hints from  $k$  clusters with low-entropy. All images are attacked to `golf-cart`. Second and Fourth row visualize our cluster segments, with darker colors representing higher mean entropy and red dots representing the location we sample hints from. Sampling hints across more clusters gives less color variety.

but they prove to be difficult with a long optimization time. Jointly attacking both hints and mask is more efficient and provides better results.

**Control over colorization.** Current attack methods lack control over where the attack occurs, opting to attack all pixels indiscriminately. This lack of control is not important for most attacks where the  $\epsilon$  is small but is concerning in cAdv where making inconsiderate large changes can be jarring. To produce realistic colorization, we need to avoid making large color changes at locations where colors are unambiguous (e.g. roads in general are gray) and focus on those where colors are ambiguous (e.g. an umbrella can have different colors). To do so, we need to segment an image and determine which segments should be attacked or preserved.

To segment the image into meaningful areas, we cluster the image’s ground truth AB space using K-Means. We first use a Gaussian filter of  $\sigma = 3$  to smooth the AB channels and then cluster them into 8 clusters. Then, we have to determine which cluster’s colors should be preserved. Fortunately, Zhang et al’s network output a per-pixel color distribution for a given image which we used to calculate the entropy of each pixel. The entropy represents how confident the network is at assigning a color at that location. The average entropy of each cluster represents how ambiguous their color is. We want to avoid making large changes to clusters with low-entropy while allowing our attack to change clusters with high entropy. One way to enforce this behavior is through hints which are sampled from the ground truth at locations belonging to clusters of low-entropy. We sample hints from the  $k$  clusters with the lowest entropy which we refer as  $\text{cAdv}_k$  (e.g.  $\text{cAdv}_2$  samples hints from the 2 lowest

entropy clusters).

**Smooth cAdv perturbations.** Fig. 2 shows interesting properties of the adversarial colors. We observe that cAdv perturbations are locally smooth and are relatively low-frequency. This is different from most adversarial attacks that generate high-frequency noise-like perturbations. This phenomenon can be explained by the observation that colors are usually smooth within object boundaries. The pretrained colorization model will thus produce smooth, low-frequency adversarial colors that often conform to object boundaries.

## 5. Experimental Results

In this section, we evaluate the two proposed attack methods both quantitatively, via attack success rate under different settings, and qualitatively, based on interesting case studies. We conduct our experiments on ImageNet [7] by randomly selecting images from 10 sufficiently different classes for the classification attack and randomly chosen images from MSCOCO [24] for image captioning attack.

### 5.1. Experimental Setup

#### 5.1.1 tAdv Attack

**Texture Features.** For texture transfer, we extract cross-layer statistics in Eq. 2 from R11, R21, R31, R41, and R51 of a pretrained VGG19 by adding a cross-entropy based adversarial loss in Eq. 1. We optimize our objective using an L-BFGS [25] optimizer.

**Number of iterations.** tAdv attacks are sensitive and if not controlled well, images get transformed into artistic images. Since we do not have any constraints over the perturbation norm, it is necessary to decide when to stop the texture transfer procedure. For a successful attack (images look realistic), we limit our L-BFGS to fixed number of small steps and perform two set of experiments: one with only one iteration or round of L-BFGS for 14 steps and another with three iterations of 14 steps. For the three iterations set up, after every iteration, we look at the confidence of our target class and stop if the confidence is greater than 0.9.

**Texture and Cross-Entropy Weights.** Empirically, we found setting  $\alpha$  to be in the range [150, 1000] and  $\beta$  in the range  $[10^{-4}, 10^{-3}]$  to be successful and also produce less perceptible tAdv examples. The additional cross-entropy based adversarial objective  $J_{adv}(I_v, t)$  helps our optimization. We ensure large flow of gradients is from the texture loss and they are sufficiently larger than the adversarial cross-entropy objective. The adversarial objective also helps in transforming victim image to adversarial without stylizing the image.

All our numbers are shown for one iteration,  $\alpha = 250$  and  $\beta = 10^{-3}$ , unless otherwise stated. We use the following annotation  $\text{tAdv}_\alpha^{iter}$  for the rest of the paper to denote the texture method that we are using.



Figure 6: **Variation in cAdv with number of color hints.** All images are attacked to *Merganser* with  $k = 4$ . As the number of hints increases, the output colors are more similar to groundtruth. However, when the number of hints is too high, colorizations might appear unrealistic.

### 5.1.2 cAdv Attack

We use Adam Optimizer [20] with a learning rate of  $10^{-4}$  in cAdv. We update hints and mask until our image reaches the target class and the confidence change of subsequent iterations does not exceed a threshold of 0.05.

**Number of input hints.** Network hints constrain our output to have similar colors as the ground truth, avoiding the possibility of unnatural colorization at the cost of color diversity. This trade-off is controlled by the number of hints provided to the network as initialization (see Fig. 6). Generally, providing more hints gives us colors similar to the original image. However, having too many hints may instead make the image less realistic as we are constraining the search space for adversarial colors.

**Number of Clusters.** The trade-off between the color diversity and the color realism is controlled by the number of clusters we sample hints from as shown in Fig. 5. Sampling from multiple clusters gives us realistic colors closer to the ground truth image at the expense of color diversity.

**Diversity vs Realism.** One of the most important factors we consider for colorization is this trade-off between color diversity and color realism. Our numbers in Table 2, 3, 7 reveal that cAdv examples with larger color changes (consequently more color diversity) are more robust against transferability and adversarial defenses. However, these big changes are found to be slightly less realistic from our user study (Table 4). Empirically, our experiments showed that in terms of color diversity, realism, and robustness of attacks, using  $k = 4$  and 50 hints works the best. For the rest of this paper, we will fix 50 hints for all  $\text{cAdv}_k$  methods.

## 5.2. Attacking Classifiers

We use a pretrained ResNet 50 classifier [15] for all our methods. DenseNet 121 [17] and VGG 19 [27] are used for our transferability analysis.

### 5.2.1 tAdv attack

**Attack Success.** With a very small weighted adversarial cross-entropy objective and using our texture loss, we break the state of the art image classifiers and yet our images look quite realistic to humans. As shown in Table 1, our attacks

	Model	Resnet50	Dense121	VGG 19
	Accuracy	76.15	74.65	74.24
Attack Success	$\text{tAdv}_{250}^1$	97.99	99.72	99.50
	$\text{tAdv}_{500}^1$	99.27	99.83	99.83
	$\text{cAdv}_1$	99.72	99.89	99.89
	$\text{cAdv}_4$	99.78	99.83	100.00

Table 1: **Whitebox Target Attack Success Rate.** Our attacks are highly successful on ResNet50, DenseNet121 and VGG19. For tAdv we show results for  $\alpha = \{250, 500\}$  and  $\beta = 0.001$ . For cAdv, we show results for  $k = \{1, 4\}$  when attacked with 50 hints.

are highly successful on white-box attacks tested on three different models with the nearest neighbor texture transfer approach. In Table 2 we show our attacks are also more transferable to other models. In our supplementary, we have results for untargeted attacks and other strategies that we used for generating tAdv adversarial examples.

**Importance of Texture in Classification.** Textures are crucial descriptors for the task of image classification. More recently, Geirhos et al. [13] showed that ImageNet-trained deep learning classifiers are biased towards texture for making predictions. From our results, it is also evident that even with a small but invisible change in the texture field can break the current state of the art classifiers.

### 5.2.2 cAdv Attack

As shown in Table 1, cAdv can achieve high targeted attack success rate by adding realistic colorization perturbation. **Importance of color in classification.** From Fig. 4, we can compare how different target class affects our colorization results if we relax our constraints on colors (cAdv on Network Weights, 0 hints). In many cases, the images contain strong colors that are related to the target class. In the case of golf-cart, we get a green tint over the entire image. This can push the target classifier to misclassify the image as green grass is usually overabundant in benign golf-cart images. Fig. 4b shows our attack on an image of a car to tench (a type of fish). We observe that the gray road turned blue and that the colors are tinted. We can hypothesize that the blue colors and the tint fooled the classifier into thinking the image is a tench in the sea.

The colorization model is originally trained to produce natural colorization that conforms to object boundaries. By adjusting its parameters, we are able to produce such large and abnormal color change that is impossible with our attack on hints and mask. These colors, however, give us some evidence that colors play a stronger role in classification than we thought. We reserve the exploration of this observation for future works.

While this effect (i.e. strong color correlation to target

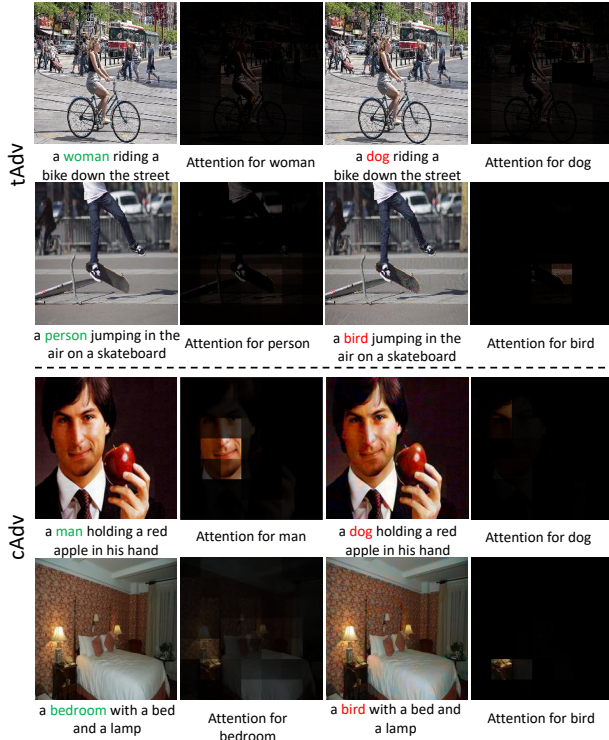


Figure 7: **Captioning attack.** We attack the second word of each caption to {dog, bird} and show the corresponding change in attention mask of that word.

class) is less pronounced for our attack on hints and mask, for all methods, we observe isoluminant color blobs in our images. Isoluminant colors are characterized by a change in color without a corresponding change in luminance. As most color changes occur along edges in natural images, it is likely that a classifier trained on ImageNet have never seen isoluminant colors. This suggests that cAdv might be exploiting isoluminant colors to fool classifiers.

### 5.3. Attacking Captioning Model

Our methods are general and can be easily adapted for other learning tasks. As proof of concept, we test our attacks against image captioning models. Image captioning is the task of generating a sequence of word description for an image. The popular architecture for captioning is a Long-Short-Term-Memory (LSTM) [16] based models [19, 28]. Recently, Janeja *et al.* proposed a convolutional based captioning model for a fast and accurate caption generation [2]. This convolutional based approach does not suffer from the commonly known problems of vanishing gradients and overly confident predictions of LSTM network. Therefore, we chose to attack the current state of the art convolutional captioning model.

Attacking captioning models is harder than attacking classifiers when the goal is to change exactly one word in the

Method	Model	ResNet50	DenseNet121	VGG19
BIM	ResNet50	100.00	17.33	12.95
	CW	98.85	16.50	11.00
tAdv <sup>1</sup> <sub>250</sub>	Resnet50	99.00	24.51	34.84
	DenseNet121	21.16	99.83	32.56
	VGG19	20.21	24.40	99.89
cAdv <sub>4</sub>	Resnet50	99.83	28.56	31.00
	DenseNet121	18.13	99.83	29.43
	VGG19	22.94	26.39	100.00

Table 2: **Transferability of attacks.** We show attack success rate of attacking models in column and testing on rows.

benign image’s caption. We show that our attacks are successful and has no visible artifacts even for this challenging task. In Fig. 7, we change the second word of the caption to {dog, bird} while keeping the rest of the caption the same. This is a challenging targeted attack because, in many untargeted attacks, the attacked captions do not make sense. For tAdv, we select  $T_S$  as the nearest neighbor of the victim image from the ones in the adversarial target class using ImageNet dataset. For cAdv, we use all ground truth hints as initialization to ensure that the attack looks realistic at a certain cost of color diversity.

### 5.4. Defense and Transferability Analysis

We evaluate our attacks and compare them with existing methods on three main defenses – JPEG defense [6], feature squeezing [31] and adversarial-training [14]. By leveraging JPEG compression and decompression, adversarial noise may be removed. We tested our methods against JPEG compression of 75. Feature squeezing is a family of simple but surprisingly effective strategies, including reducing color bit depth and spatial smoothing. It has been shown that this can defend various adversarial attacks without harming the benign accuracy. By coalescing feature vectors, it essentially shrinks the search space available for the adversary, making it harder to search for perturbation. Adversarial training has been shown as an effective but costly method to defend against adversarial attacks.

**Robustness of Our Attacks.** In general, our attacks are more robust to the considered defenses and transferable when compared with three popular attack methods FGSM [14] BIM [22] and CW [4]. Our untargeted analysis, including FGSM, can be found in supplementary. For tAdv, increasing texture weight does not necessarily perform well with the defense even though it increases attack success rate, but increasing texture flow with more subsequent iterations improves attack’s robustness against defenses. For cAdv, there is a trade-off between more realistic colors (using more hints and sampling from more clusters) and attack robustness. From Table 3 and 2, we show that as we progressively use more clusters, our transferability and defense numbers drop. A similar trend is observed with the change in the number of hints (see supplementary).

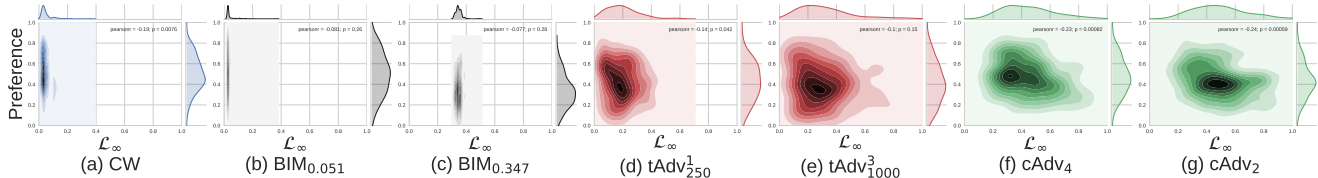


Figure 8: **Density Plot.** Our methods achieve large  $\mathcal{L}_\infty$  norm perturbations without notable reduction in user preference. Each plot is a density plot between perturbation ( $\mathcal{L}_\infty$  norm) on X axis and  $Pr(\text{user prefers adversarial image})$  on Y axis. For ideal systems, the density would be a concentrated horizontal line at 0.5. All plots are on the same set of axes. On the **left**, plots for three baseline methods (Fig a - Fig c). Note the very strong concentration on small norm perturbations, which users like. **Right** 4 plots shows our methods (Fig d - Fig g). Note strong push into large norm regions, without loss of user preference.

Method	JPEG75	Feature Squeezing					Adv Trained Resnet
		4-bit	5-bit	2x2	3x3	11-3-4	
BIM	<b>12.73</b>	<b>28.62</b>	<b>86.66</b>	<b>34.28</b>	<b>21.56</b>	<b>29.28</b>	<b>19.28</b>
CW	11.50	12.00	30.50	22.00	14.50	18.50	19.50
tAdv <sub>250</sub> <sup>1</sup>	32.89	62.79	89.743	54.94	38.92	40.57	27.41
tAdv <sub>250</sub> <sup>2</sup>	<b>36.33</b>	<b>67.68</b>	<b>94.11</b>	<b>58.92</b>	<b>42.82</b>	44.56	<b>29.01</b>
tAdv <sub>1000</sub> <sup>1</sup>	31.49	52.69	90.52	51.24	34.85	39.68	27.27
tAdv <sub>1000</sub> <sup>3</sup>	35.23	61.40	93.18	56.31	39.66	<b>45.59</b>	26.24
cAdv <sub>1</sub>	<b>52.33</b>	<b>47.78</b>	<b>76.17</b>	<b>36.28</b>	<b>50.50</b>	<b>61.95</b>	<b>41.44</b>
cAdv <sub>4</sub>	42.61	38.39	69.67	34.34	40.78	54.62	31.94
cAdv <sub>8</sub>	38.22	36.62	67.06	31.67	37.67	49.17	27.17

Table 3: **Defense.** Misclassification rate after passing through defense models. All attacks are done on ResNet50. The highest success rate of each group of methods is in bold.

## 6. Human Perceptual Study

To quantify how realistic tAdv and cAdv examples are, we conducted a user study on Amazon Mechanical Turk. For each attack, we choose the same 200 adversarial images and their corresponding benign ones. During each trial, one random adversarial-benign pair appears for three seconds and workers are given five minutes to identify the realistic one. Each attack has 600 unique pairs of images and each pair is evaluated by at least 10 unique workers. We restrict biases in this process by allowing each unique user up to 5 rounds of trials. In total, 598 unique workers completed at least one round of our user study. For each image, we can then calculate the user preference score as the number of times it is chosen divided by the number of times it is displayed. 0.5 represents that users are unable to distinguish if the image is fake.

For baselines, we chose BIM and CW. Since these attacks are known to have low  $\mathcal{L}_p$  norm, we designed an aggressive version of BIM by relaxing its  $\mathcal{L}_\infty$  bound to match the norm of our attacks. We settled with two aggressive versions of BIM with average  $\mathcal{L}_\infty = \{0.21, 0.347\}$ , which we refer to as BIM<sub>0.21</sub>, BIM<sub>0.34</sub>.

**Results.** The user preferences for all attacks are summarized in Table 4. For tAdv and cAdv, user preferences averages at 0.433 and 0.476 respectively, indicating that workers have a hard time distinguishing them. The average user preferences for BIM drops drastically from 0.497 to 0.332 when we relax the norm to BIM<sub>0.34</sub>; the decrease in user preferences for tAdv (0.433 to 0.406) and cAdv (0.476 to 0.437) is not

Method	$\mathcal{L}_0$	$\mathcal{L}_2$	$\mathcal{L}_\infty$	Preference
cw	0.587	0.026	0.054	0.506
BIM <sub>0.051</sub>	0.826	0.030	0.051	0.497
BIM <sub>0.21</sub>	0.893	0.118	0.21	0.355
BIM <sub>0.347</sub>	0.892	0.119	0.347	0.332
tAdv <sub>250</sub> <sup>1</sup>	0.891	0.041	0.198	0.433
tAdv <sub>1000</sub> <sup>1</sup>	0.931	0.056	0.237	0.412
tAdv <sub>250</sub> <sup>3</sup>	0.916	0.061	0.258	0.425
tAdv <sub>1000</sub> <sup>3</sup>	0.946	0.08	0.315	0.406
cAdv <sub>2</sub>	0.910	0.098	0.489	0.437
cAdv <sub>4</sub>	0.898	0.071	0.448	0.473
cAdv <sub>8</sub>	0.896	0.059	0.425	0.476

Table 4: **User Study.** User preference score and  $\mathcal{L}_p$  norm of perturbation for different attacks. tAdv and cAdv are imperceptible for humans (score close to 0.5) even with very big  $\mathcal{L}_p$  norm perturbation.

significant. In Fig. 8 and Fig. 11, we show density plot of  $\mathcal{L}_p$  norm vs user preference scores.

## 7. Discussion and Conclusion

We propose two novel attacks based on semantic manipulation to generate realistic adversarial examples, departing from previous works that limit the  $\mathcal{L}_p$  norm of perturbations. Our user study shows that despite having unbounded  $\mathcal{L}_p$  norm, the adversarial images generated by our methods are able to consistently fool human subjects. Our attacks also shed light on the role of texture and color fields in influencing deep network’s predictions. From the density plot in Fig. 8, the correlation between user preferences and  $\mathcal{L}_\infty$  for cAdv is weak ( $\approx 0$ ) for both cAdv<sub>4</sub> and cAdv<sub>2</sub> even with a large  $\mathcal{L}_\infty = 0.489$ . These are very large  $\mathcal{L}_\infty$  norm perturbations that maintain the property of being a natural image (for example, make the blue umbrella red in Fig. 5). Such perturbations are very hard to find from other methods that control  $\mathcal{L}_\infty$  norm. These results also dispute the belief of our community that small magnitude perturbation is required to generate photorealistic adversarial examples. We hope by presenting our methods, we encourage future studies on unbounded adversarial attacks, better metrics for measuring perturbations, and more sophisticated defenses.

## Supplementary Material

**Adversarial Cross-Entropy Objective for Captions.** Let  $t$  be the target caption,  $w$  denote the word position of the caption,  $\mathcal{F}$  for the captioning model,  $I_v$  for the victim image.

$$L_{capt}^A = \sum_w J_{adv}((\mathcal{F}(I_v))_w, t_w) \quad (6)$$

For **tAdv**, we add this cross-entropy to our texture perturbation loss and directly optimize the image to generate target captions. For **cAdv**, we give all color hints and optimize to get an adversarial colored image to produce target caption. We stop our attack once we reach the target caption and the caption doesn't change with subsequent iterations. Note we do not attack or optimize the network weights, we only optimize the victim image (for **tAdv**) or hints and mask (for **cAdv**) to achieve our target.

	Model	Resnet50	Dense121	VGG 19
	Accuracy	76.15	74.65	74.24
Attack Success	Random $T_s$	99.67	99.72	96.16
	Random Target $T_s$	99.72	99.89	99.94
	Nearest Target $T_s$	97.99	99.72	99.50
	cAdv <sub>4</sub> 25 hints	99.78	99.83	99.93
	cAdv <sub>4</sub> 50 hints	99.78	99.83	100.00
	cAdv <sub>4</sub> 100 hints	99.44	99.50	99.93

Table 5: **Whitebox target attack success rate.** Our attacks are highly successful on different models across all strategies. **tAdv** results are for  $\alpha = 250$ ,  $\beta = 10^{-3}$  and iter= 1.

$\beta \backslash \alpha$	250	500	750	1000
$10^{-4}$	99.88	99.61	98.55	95.92
$10^{-3}$	97.99	99.27	99.66	99.50
$10^{-2}$	96.26	95.42	96.32	96.59

Table 6: **tAdv ablation study.** Whitbox target success rate with nearest target  $T_s$  (texture source). In columns, we have increasing texture weight ( $\alpha$ ) and in rows, we have increasing adversarial cross-entropy weight ( $\beta$ ). All attacks are done with one iteration of L-BFGS of 14 steps on Resnet50. We found  $\alpha \leq 500$  and  $\beta = 10^{-3}$  to produce more imperceptible and robust adversarial examples.

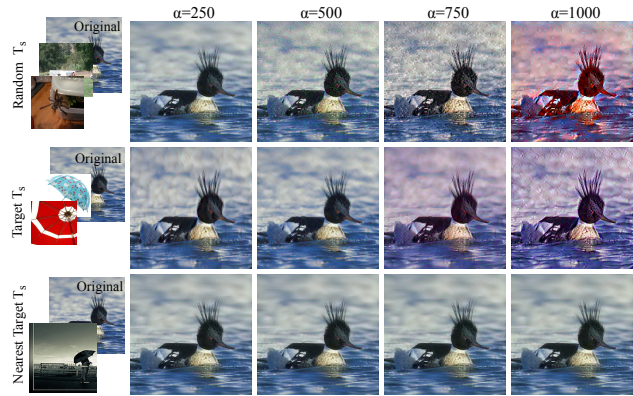


Figure 9: **Additional qualitative examples for tAdv.** Texture transferred from random “texture source” ( $T_s$ ) in row 1, random target class  $T_s$  (row 2) and from the nearest target class  $T_s$  (row 3). All examples are misclassified from Merganser to Umbrella. Images in the last row look more natural, while those in the first two rows contain more artifacts as the texture weight  $\alpha$  increases (from left to right).

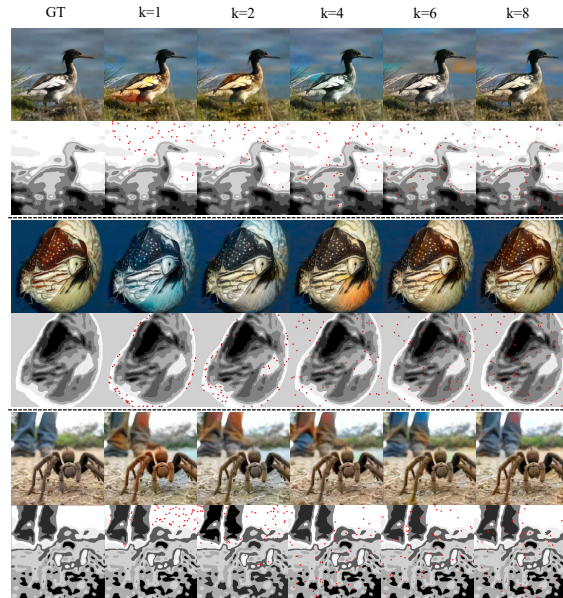


Figure 10: **Additional qualitative examples for controlling cAdv.** We show a comparison of sampling 50 color hints from  $k$  clusters with low-entropy. All images are attacked to golf-cart. Even numbered rows visualize our cluster segments, with darker colors representing higher mean entropy and red dots representing the location we sample hints from. Sampling hints across more clusters gives less color variety.

Targeted Method	Strategy	JPEG75	Feature Squeezing					Adv Trained Resnet	
			4-bit	5-bit	2x2	3x3	11-3-4		
BIM		12.73	<b>28.62</b>	<b>86.66</b>	<b>34.28</b>	<b>21.56</b>	<b>29.28</b>	19.28	
CW		11.50	12.00	30.50	22.00	14.50	18.50	<b>19.50</b>	
$tAdv_{250}^1$	Random $T_s$	39.67	65.42	84.10	56.20	42.84	44.71	<b>27.29</b>	
	Random Target $T_s$	<b>44.95</b>	<b>70.00</b>	85.45	<b>60.15</b>	<b>47.37</b>	<b>47.73</b>	26.96	
$tAdv_{250}^1$	Nearest Target $T_s$	32.89	62.79	89.743	54.94	38.92	40.57	27.41	
$tAdv_{250}^3$		<b>36.33</b>	<b>67.68</b>	<b>94.11</b>	<b>58.92</b>	<b>42.82</b>	44.56	<b>29.01</b>	
$tAdv_{1000}^1$		31.49	52.69	90.52	51.24	34.85	39.68	27.27	
$tAdv_{1000}^3$		35.23	61.40	93.18	56.31	39.66	<b>45.59</b>	26.24	
$cAdv_4$	25 Hints	<b>45.78</b>	<b>43.06</b>	<b>72.39</b>	34.00	<b>44.78</b>	<b>55.28</b>	<b>34.50</b>	
	50 Hints	42.61	38.39	69.67	<b>34.34</b>	40.78	54.62	31.94	
	100 Hints	39.56	36.83	67.00	31.06	37.94	50.72	29.28	
$cAdv_1$	50 Hints	<b>52.33</b>	<b>47.78</b>	<b>76.17</b>	<b>36.28</b>	<b>50.50</b>	<b>61.95</b>	<b>41.44</b>	
$cAdv_2$		46.61	42.78	72.56	34.28	46.45	59.00	36.56	
$cAdv_8$		38.22	36.62	67.06	31.67	37.67	49.17	27.17	
Untargeted									
FGSM		78.49	83.50	87.00	80.50	82.50	82.00	35.5	
$tAdv_{250}^1$	Nearest Target $T_s$	<b>52.31</b>	<b>88.00</b>	96.00	<b>72.50</b>	<b>58.50</b>	<b>59.00</b>	26.50	
		$tAdv_{500}^1$	50.77	84.50	<b>97.00</b>	70.00	56.50	58.00	<b>29.00</b>
		$tAdv_{1000}^1$	45.13	82.50	96.50	65.00	53.00	53.00	27.50
$cAdv_1$	50 Hints	<b>75.22</b>	<b>64.06</b>	<b>87.78</b>	<b>42.33</b>	<b>65.45</b>	<b>70.00</b>	<b>35.70</b>	
$cAdv_4$		69.17	57.67	84.56	39.89	62.83	66.12	31.95	
$cAdv_8$		66.50	55.94	85.12	39.73	60.72	62.56	26.56	

Table 7: Attack success (or misclassification) rate after passing through defense models. All “Targeted Attacks” comparison are at the top of the table, and “Untargeted Attacks” comparison are at the bottom of the table. All attacks are done on ResNet50. Highest attack success rate of each group of method is in bold. For  $tAdv$ , all numbers are reported for  $\beta = 10^{-3}$ .

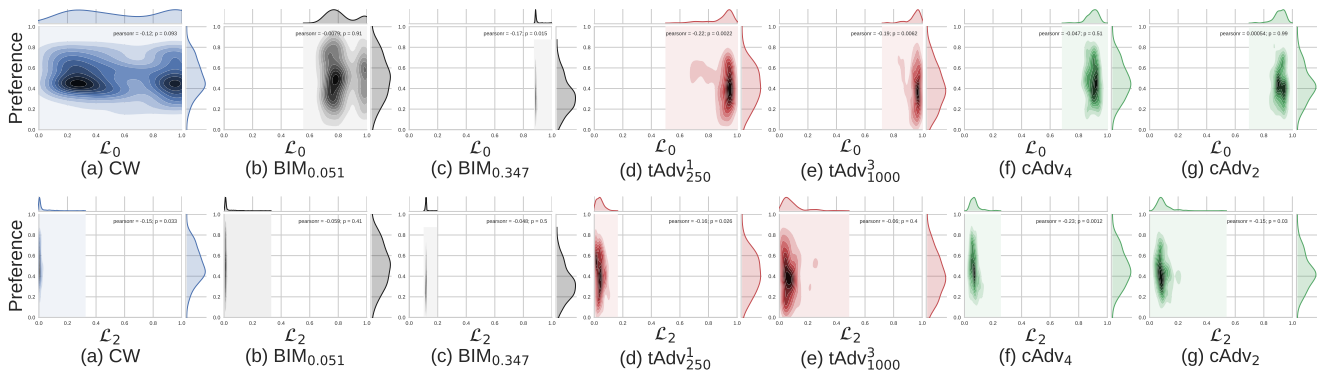
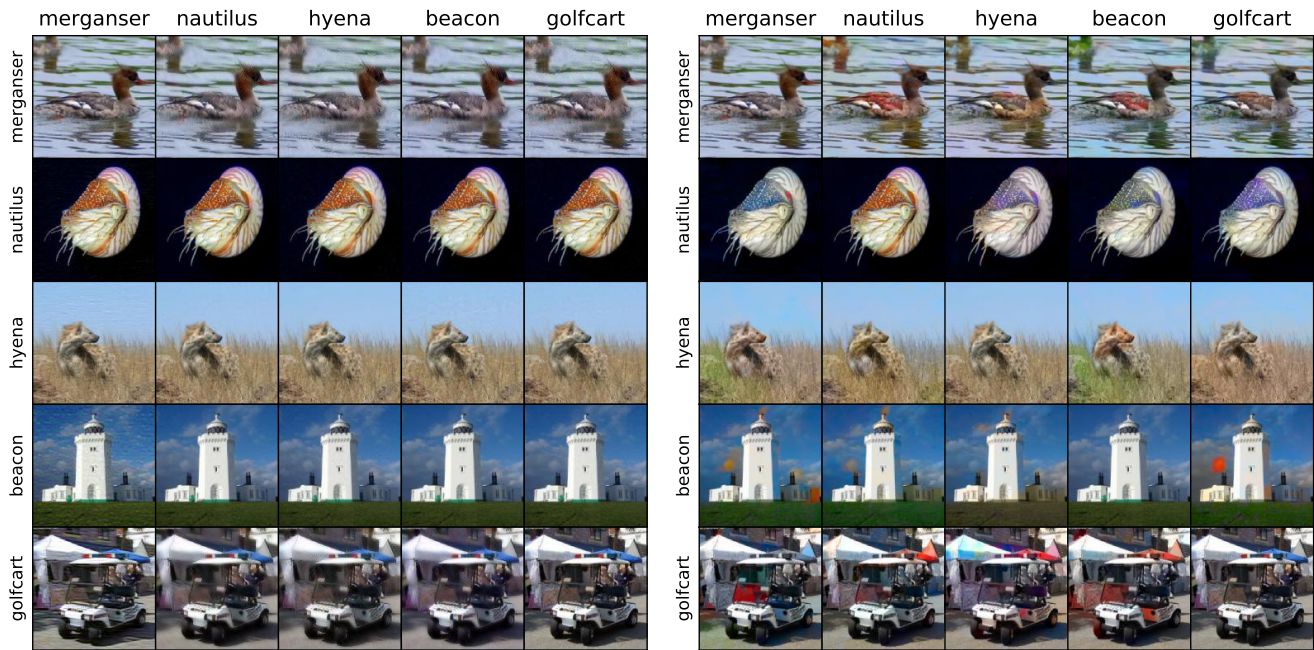


Figure 11: **Density Plot.** Our methods achieve large  $\mathcal{L}_0$  norm (top) and  $\mathcal{L}_2$  norm (bottom) norm perturbations without notable reduction in user preference. Each plot is a density plot between perturbation ( $\mathcal{L}_p$  norm) on X axis and  $Pr(\text{user prefers adversarial image})$  on Y axis. For ideal systems, the density would be a concentrated horizontal line at 0.5. All plots are on the same set of axes. On the **left**, plots for three baseline methods (Fig a - Fig c). Note the very strong concentration on small norm perturbations, which users like. **Right** 4 plots shows our methods (Fig d - Fig g). Note strong push into large norm regions, without loss of user preference.

Attack		tarantula	merganser	nautilus	hyena	beacon	golfcart	photocopier	umbrella	pretzel	sandbar	Mean
BIM	$\mathcal{L}_0$	0.82	0.81	0.80	0.88	0.80	0.79	0.86	0.80	0.85	0.84	0.83
	$\mathcal{L}_2$	0.05	0.02	0.03	0.04	0.02	0.01	0.04	0.02	0.02	0.04	0.03
	$\mathcal{L}_\infty$	0.07	0.04	0.06	0.06	0.04	0.03	0.07	0.04	0.04	0.06	0.05
	Preference	0.49	0.75	0.44	0.67	0.48	0.48	0.27	0.39	0.38	0.63	0.50
CW	$\mathcal{L}_0$	0.54	0.55	0.52	0.77	0.48	0.42	0.70	0.48	0.69	0.71	0.59
	$\mathcal{L}_2$	0.05	0.01	0.03	0.03	0.02	0.01	0.04	0.01	0.02	0.04	0.03
	$\mathcal{L}_\infty$	0.08	0.04	0.06	0.07	0.04	0.03	0.07	0.04	0.05	0.06	0.05
	Preference	0.51	0.68	0.43	0.59	0.52	0.51	0.39	0.40	0.42	0.62	0.51
tAdv <sub>250</sub> <sup>3</sup>	$\mathcal{L}_0$	0.94	0.95	0.91	0.94	0.89	0.94	0.89	0.91	0.94	0.85	0.92
	$\mathcal{L}_2$	0.07	0.08	0.08	0.06	0.05	0.06	0.03	0.05	0.07	0.05	0.06
	$\mathcal{L}_\infty$	0.28	0.31	0.30	0.31	0.22	0.27	0.18	0.25	0.27	0.19	0.26
	Preference	0.39	0.58	0.43	0.53	0.46	0.35	0.25	0.40	0.33	0.54	0.43
cAdv <sub>4</sub>	$\mathcal{L}_0$	0.90	0.90	0.88	0.90	0.90	0.90	0.90	0.89	0.93	0.88	0.90
	$\mathcal{L}_2$	0.06	0.06	0.07	0.05	0.08	0.07	0.08	0.08	0.09	0.06	0.07
	$\mathcal{L}_\infty$	0.36	0.44	0.41	0.31	0.48	0.51	0.55	0.56	0.46	0.39	0.45
	Preference	0.46	0.65	0.46	0.58	0.45	0.48	0.30	0.43	0.35	0.59	0.47

Table 8: Class-wise  $\mathcal{L}_p$  norm and user preferences breakdown. Perturbations for a few classes (e.g. photocopier) are quite obvious and easy to detect for all methods, and much harder for a few classes (e.g. merganser).



(a) tAdv<sub>250</sub><sup>1</sup> for nearest Target  $T_s$

(b) cAdv<sub>4</sub> with 50 hints

Figure 12: Randomly sampled tAdv and cAdv adversarial examples. (a) Adversarial examples generated by tAdv with  $\alpha = 250$ ,  $\beta = 10^{-3}$  and iter= 1 using nearest target  $T_s$ . (b) Adversarial examples generated by cAdv attacking Hints and mask with 50 hints. Note diagonal images are ground truth images and gray pixels indicate no perturbation.

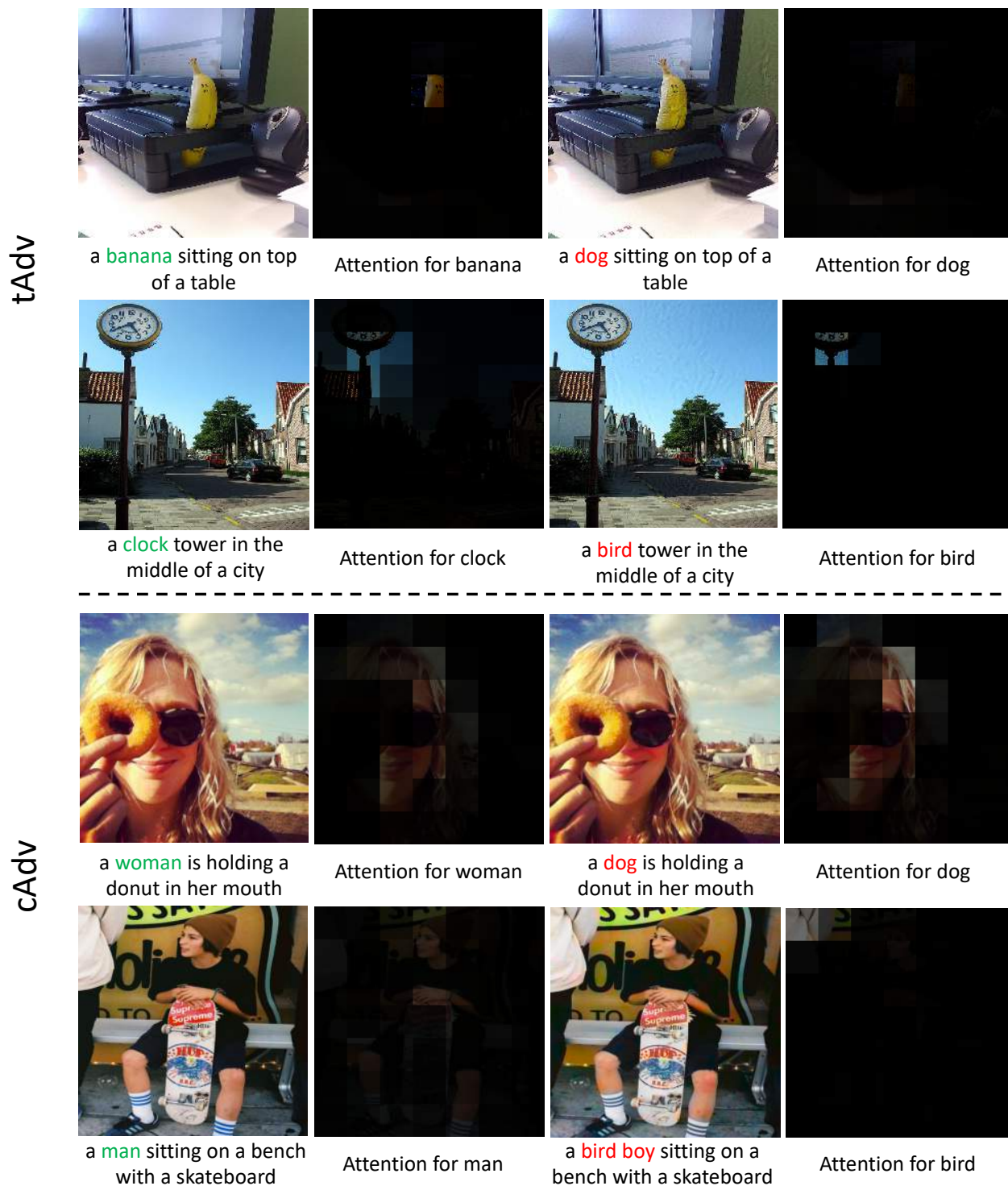


Figure 13: **Additional example for Captioning attack.** We attack the second word of each caption to {dog, bird} and show the corresponding change in attention mask of that word. For tAdv we use the nearest neighbor selection method and for cAdv we initialize with all groundtruth color hints.

## References

- [1] Introducing the unrestricted adversarial examples challenge. <https://ai.googleblog.com/2018/09/introducing-unrestricted-adversarial.html>. Accessed: 2018-09-13. **2**
- [2] J. Aneja, A. Deshpande, and A. G. Schwing. Convolutional image captioning. In *Proceedings of the IEEE Conference on Computer Vision and Pattern Recognition*, pages 5561–5570, 2018. **2, 7**
- [3] A. N. Bhagoji, W. He, B. Li, and D. Song. Exploring the space of black-box attacks on deep neural networks. *arXiv preprint arXiv:1712.09491*, 2017. **1**
- [4] N. Carlini and D. Wagner. Towards evaluating the robustness of neural networks. In *2017 IEEE Symposium on Security and Privacy (SP)*, pages 39–57. IEEE, 2017. **1, 2, 7**
- [5] M. Cimpoi, S. Maji, I. Kokkinos, S. Mohamed, and A. Vedaldi. Describing textures in the wild. In *Proceedings of the IEEE Conference on Computer Vision and Pattern Recognition*, pages 3606–3613, 2014. **3**
- [6] N. Das, M. Shanbhogue, S.-T. Chen, F. Hohman, L. Chen, M. E. Kounavis, and D. H. Chau. Keeping the bad guys out: Protecting and vaccinating deep learning with jpeg compression. *arXiv preprint arXiv:1705.02900*, 2017. **7**
- [7] J. Deng, W. Dong, R. Socher, L.-J. Li, K. Li, and L. Fei-Fei. ImageNet: A Large-Scale Hierarchical Image Database. In *CVPR09*, 2009. **2, 5**
- [8] A. Deshpande, J. Lu, M.-C. Yeh, M. J. Chong, and D. A. Forsyth. Learning diverse image colorization. In *CVPR*, pages 2877–2885, 2017. **3**
- [9] A. A. Efros and W. T. Freeman. Image quilting for texture synthesis and transfer. In *Proceedings of the 28th annual conference on Computer graphics and interactive techniques*, pages 341–346. ACM, 2001. **3**
- [10] K. Eykholt, I. Evtimov, E. Fernandes, B. Li, A. Rahmati, C. Xiao, A. Prakash, T. Kohno, and D. Song. Robust physical-world attacks on deep learning visual classification. In *Proceedings of the IEEE Conference on Computer Vision and Pattern Recognition*, pages 1625–1634, 2018. **1**
- [11] L. Gatys, A. S. Ecker, and M. Bethge. Texture synthesis using convolutional neural networks. In *Advances in Neural Information Processing Systems*, pages 262–270, 2015. **3**
- [12] L. A. Gatys, A. S. Ecker, and M. Bethge. Image style transfer using convolutional neural networks. In *Proceedings of the IEEE Conference on Computer Vision and Pattern Recognition*, pages 2414–2423, 2016. **3**
- [13] R. Geirhos, P. Rubisch, C. Michaelis, M. Bethge, F. A. Wichmann, and W. Brendel. Imagenet-trained cnns are biased towards texture; increasing shape bias improves accuracy and robustness. *arXiv preprint arXiv:1811.12231*, 2018. **6**
- [14] I. J. Goodfellow, J. Shlens, and C. Szegedy. Explaining and harnessing adversarial examples. *arXiv preprint arXiv:1412.6572*, 2014. **2, 7**
- [15] K. He, X. Zhang, S. Ren, and J. Sun. Deep residual learning for image recognition. In *Proceedings of the IEEE conference on computer vision and pattern recognition*, pages 770–778, 2016. **6**
- [16] S. Hochreiter and J. Schmidhuber. Long short-term memory. *Neural computation*, 9(8):1735–1780, 1997. **7**
- [17] G. Huang, Z. Liu, L. Van Der Maaten, and K. Q. Weinberger. Densely connected convolutional networks. **6**
- [18] X. Huang and S. J. Belongie. Arbitrary style transfer in real-time with adaptive instance normalization. In *ICCV*, pages 1510–1519, 2017. **3**
- [19] A. Karpathy and L. Fei-Fei. Deep visual-semantic alignments for generating image descriptions. In *Proceedings of the IEEE conference on computer vision and pattern recognition*, pages 3128–3137, 2015. **7**
- [20] D. P. Kingma and J. Ba. Adam: A method for stochastic optimization. *arXiv preprint arXiv:1412.6980*, 2014. **6**
- [21] D. P. Kingma and M. Welling. Auto-encoding variational bayes. *arXiv preprint arXiv:1312.6114*, 2013. **3**
- [22] A. Kurakin, I. J. Goodfellow, and S. Bengio. Adversarial examples in the physical world. *CoRR*, abs/1607.02533, 2016. **1, 2, 7**
- [23] Y. Li, C. Fang, J. Yang, Z. Wang, X. Lu, and M.-H. Yang. Universal style transfer via feature transforms. In *Advances in Neural Information Processing Systems*, pages 386–396, 2017. **3**
- [24] T.-Y. Lin, M. Maire, S. Belongie, J. Hays, P. Perona, D. Ramanan, P. Dollár, and C. L. Zitnick. Microsoft coco: Common objects in context. In *European conference on computer vision*, pages 740–755. Springer, 2014. **2, 5**
- [25] D. C. Liu and J. Nocedal. On the limited memory bfgs method for large scale optimization. *Mathematical programming*, 45(1-3):503–528, 1989. **5**
- [26] N. Papernot, P. McDaniel, and I. Goodfellow. Transferability in machine learning: from phenomena to black-box attacks using adversarial samples. *arXiv preprint arXiv:1605.07277*, 2016. **2**
- [27] K. Simonyan and A. Zisserman. Very deep convolutional networks for large-scale image recognition. *arXiv preprint arXiv:1409.1556*, 2014. **3, 6**
- [28] L. Wang, A. Schwing, and S. Lazebnik. Diverse and accurate image description using a variational auto-encoder with an additive gaussian encoding space. In *Advances in Neural Information Processing Systems*, pages 5756–5766, 2017. **7**
- [29] C. Xiao, B. Li, J.-Y. Zhu, W. He, M. Liu, and D. Song. Generating adversarial examples with adversarial networks. *arXiv preprint arXiv:1801.02610*, 2018. **2**
- [30] C. Xiao, J.-Y. Zhu, B. Li, W. He, M. Liu, and D. Song. Spatially transformed adversarial examples. *arXiv preprint arXiv:1801.02612*, 2018. **1, 2**
- [31] W. Xu, D. Evans, and Y. Qi. Feature squeezing: Detecting adversarial examples in deep neural networks. *arXiv preprint arXiv:1704.01155*, 2017. **7**
- [32] M.-C. Yeh, S. Tang, A. Bhattad, and D. A. Forsyth. Quantitative evaluation of style transfer. *arXiv preprint arXiv:1804.00118*, 2018. **3**
- [33] R. Zhang, P. Isola, and A. A. Efros. Colorful image colorization. In *European Conference on Computer Vision*, pages 649–666. Springer, 2016. **4**
- [34] R. Zhang, J.-Y. Zhu, P. Isola, X. Geng, A. S. Lin, T. Yu, and A. A. Efros. Real-time user-guided image colorization with

learned deep priors. *arXiv preprint arXiv:1705.02999*, 2017.

3